Supporting Information

Tuning the Porosity of Supraparticles

Wendong Liu, Michael Kappl, and Hans-Jürgen Butt*

Department of Physics at Interfaces, Max Planck Institute for Polymer Research, Ackermannweg 10, D-55128 Mainz, Germany

* Correspondence and requests for materials should be addressed to M.K. (E-mail: kappl@mpip-mainz.mpg.de)

Calcination method: The temperature and time of calcination are essential parameters to control the property of supraparticles. For TiO_2 supraparticles fabrication, the tuning of porosity relies on the concentration of PS templates since the mesoporous structure is already formed during the evaporation. The TiO_2 used in this work is P25, which consists mainly of the anatase crystalline phase with high photocatalytic activity. The calcination process must avoid a crystalline transformation from anatase to rutile. Otherwise, the catalytic activity would be degraded. To identify the proper calcination conditions, we performed calcination of binary TiO_2-PS supraparticles with R equal to 1:5 with temperatures between 400 °C to 600 °C, and calcination times between 1 h to 24 h. The final supraparticle structure was characterized by SEM, while the primary TiO_2 nanoparticles after treatment at 500 °C and 600 °C for 3 h, 6 h, and 24 h were characterized by TEM and XRD. As shown in Figure S13-15, after calcination under different temperatures for a specific time, all the samples exhibited macropores with a similar size and structure from the surface to the inner part of the supraparticles. It demonstrates that the calcination step just removes the PS templates but not cause significant variation of the mesoporous structure. Even though all the samples showed macropores, the PS phase was not completely removed for the lowest temperature (400 °C) and short calcination times (1-3 h). As all the calcinations are conducted above the melting temperature of PS (~ 240 °C), the PS particles will change to fluidic state and can fill the interstitial spaces of the TiO_2 nanoparticles. The macropores could still be observed through SEM even if PS phase was not completely removed. From the optical appearance, we can conclude that the polymer residues still exists after calcination at the lowest temperature and shorter times. As shown in Figure S16f, the binary TiO_2-PS supraparticles without calcination present a milk-white color. After calcining under 400 °C for 1 h, the particles show a brown color, which is caused by the incomplete burning of the polymer phase (Figure S16a). With increasing calcination time, the color gradually becomes lighter, indicating further removal of the PS phase. After 3 h calcination at 400 °C, the particles are still slightly colored (Figure S16c). Supraparticles obtained after

calcination at 500 °C for 3 h and 6 h have the same white color as the pure TiO_2 (Figure S16d,e). This indicates that after a calcination step at 500 °C for 3 h, the polymer phase has been fully removed. Also samples after calcination at 400 °C for 6 h, 12 h, 24 h, and at 500 °C for 1 h and 2 h have fully white color. The second important parameter for choosing optimum calcination condition is a possible phase transition of TiO_2. Temperature and duration of calcination can affect the crystal phase of TiO_2 and hence its catalytic activity. To investigate such influence, binary supraparticles were calcined with prolonged calcining time of up to 24 h and enhanced temperature up to 600 °C. As shown in Figure S14 and S15, the porous structure is similar to the ones at lower temperature and shorter times, indicating that no significant structural changes happened. The structure and crystal phase of P25 after calcining at 500 °C and 600 °C were characterized by XRD and TEM. As shown in Figure S12, after 24 h calcination at 500 °C, the XRD patterns of P25 were unchanged. However, after 600 °C calcination for 3 h, the XRD pattern clearly indicate crystalline transformation from anatase to rutile. Such phase transformation will reduce the catalytic activity of the porous supraparticles due to the lower photocatalytic activity of rutile compared to anatase. No obvious sintering or size change of nanoparticles was observed in TEM images (Figure S17). These findings further support that TiO_2 nanoparticles already form stable mesoporous structures during the evaporation process. This structure will not be significantly altered during calcination far below the sintering temperature of TiO_2. Thus, for the fabrication of TiO_2 supraparticles, 500 °C for 3 h was chosen as optimum calcination condition, ensuring complete removal of PS polymer templates while maintaining the activity of primary P25 particles.

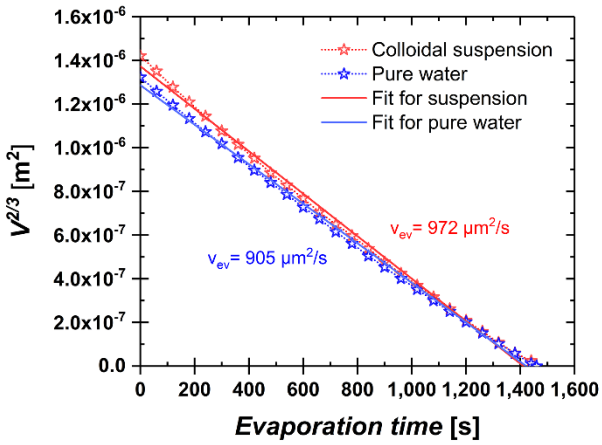

Figure S1. Relationship between droplet volume and evaporation time for pure water and the colloidal suspension. The evaporation was conducted under 22 ℃ and relative humidity RH = 40%.

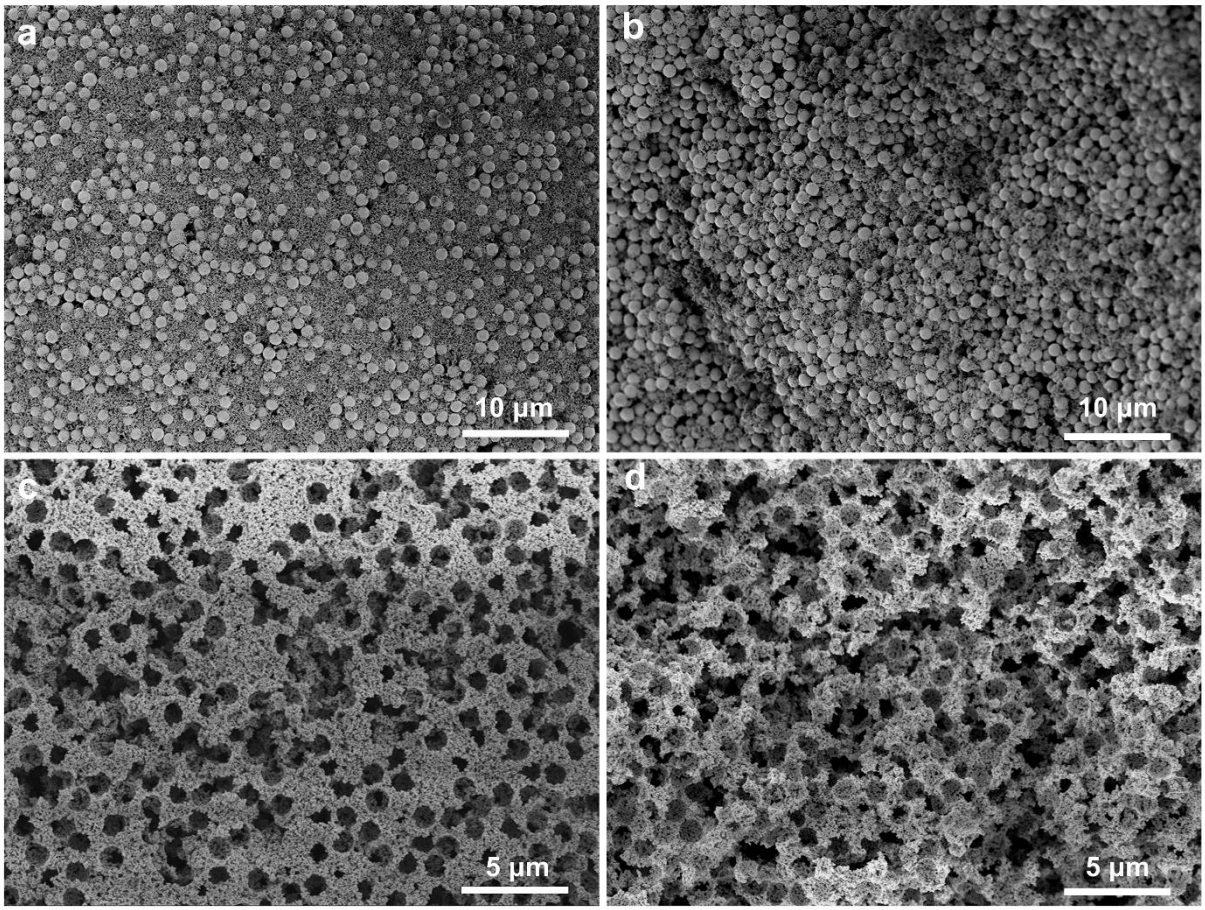

Figure S2. Supraparticles obtained after evaporation and calcination. (a-b) SEM images of the surface part (a) and the inner part (b) of TiO_2-PS binary supraparticles obtained after evaporation. (c-d) SEM images of the surface part (c) and the inner part (d) of highly porous TiO_2 supraparticles achieved after calcination.

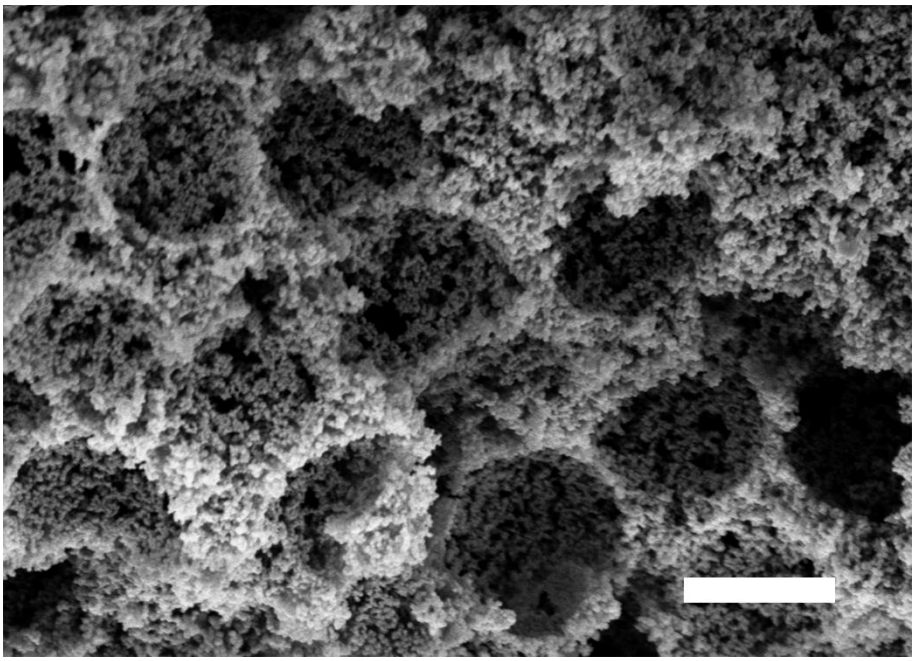

Figure S3. Enlarged SEM image of the inner structure of porous TiO_2 supraparticles. Scale bar is 1 μm.

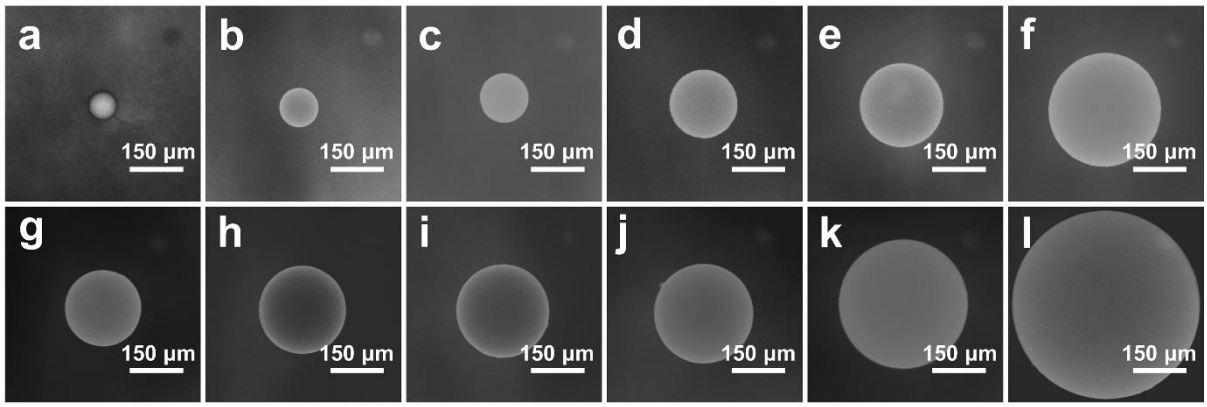

Figure S4. Optical microscope images of supraparticles with different sizes. (a-f) Porous TiO_2 supraparticles with the size controlled by the initial volume of the drop with the same particle concentration (0.1 %) (From left to right: 0.3 μL (70 μm), 0.5 μL (110 μm), 1 μL (140 μm), 2 μL (180 μm), 5 μL (240 μm), and 10 μL (320 μm)). (g-l) Porous TiO_2 supraparticles with the size controlled by the concentration of particles inside the drop and volume (From left to right: 0.2%-2 μL (210 μm), 0.3%-2 μL (240 μm), 0.4%-2 μL (260 μm), 0.5%-2 μL (280 μm), 1%-2 μL (440 μm), and 1%-5 μL (530 μm)). The scale bars indicate 150 μm.

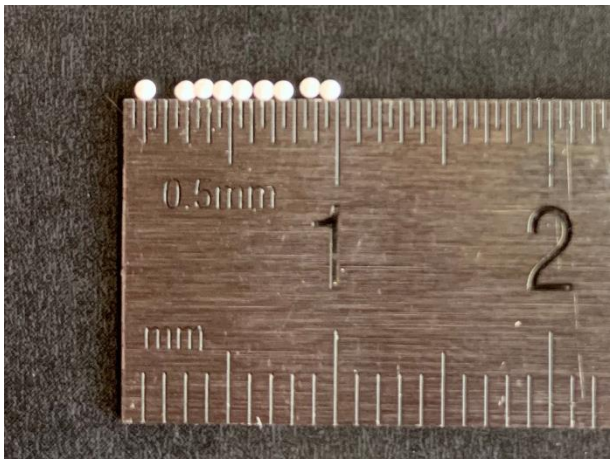

Figure S5. Optical image of large supraparticles with a size of about 900 μm. The particles were obtained by evaporating 10 μL binary colloidal droplets with a concentration of 1% (vol%).

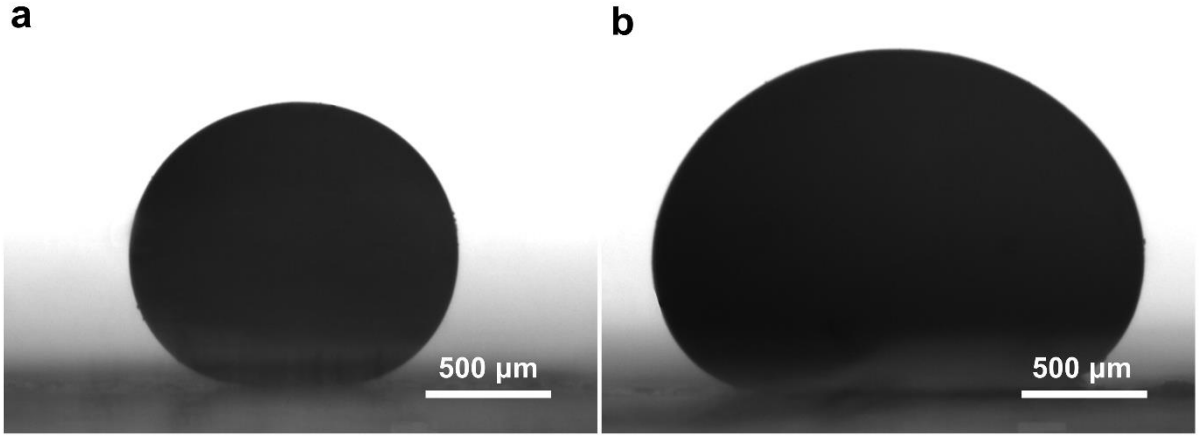

Figure S6. Side-view photographs of binary supraparticle achieved by evaporating 40 μL (a) and 100 μL (b) binary colloidal droplet with a concentration of 1% (vol%).

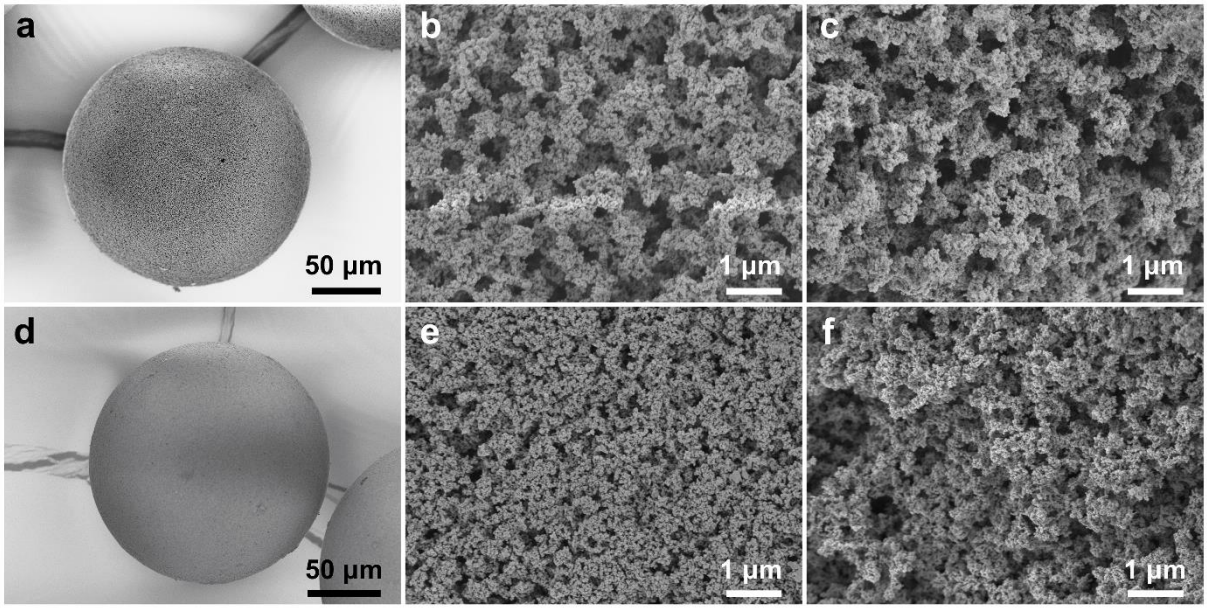

Figure S7. Porous supraparticles with regulated macro-pore sizes. (a-c) SEM images of the whole particle (a), the porous surface (b) and inner porous structure (c) of supraparticle with macropores derived from 572 nm PS nanoparticles. (d-f) SEM images of the whole particle (d), the porous surface (e) and inner porous structure (f) of supraparticle with macropores derived from 270 nm PS nanoparticles.

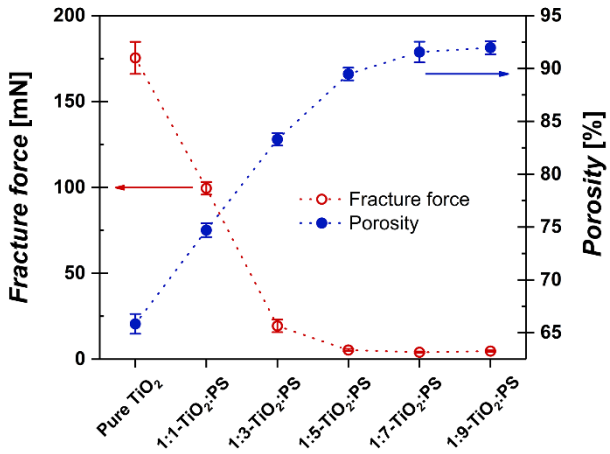

Figure S8. Mechanical stability (fracture force) and porosity of supraparticles derived from specific ratio of TiO_2-to-PS.

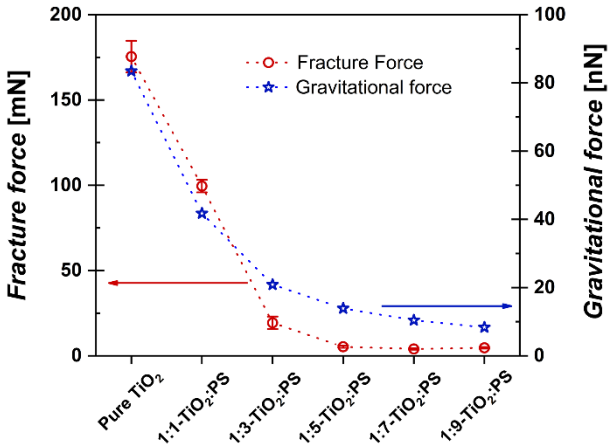

Figure S9. Comparison of fracture force with gravitational force on each porous supraparticle (note the factor 10^6 difference in scales).

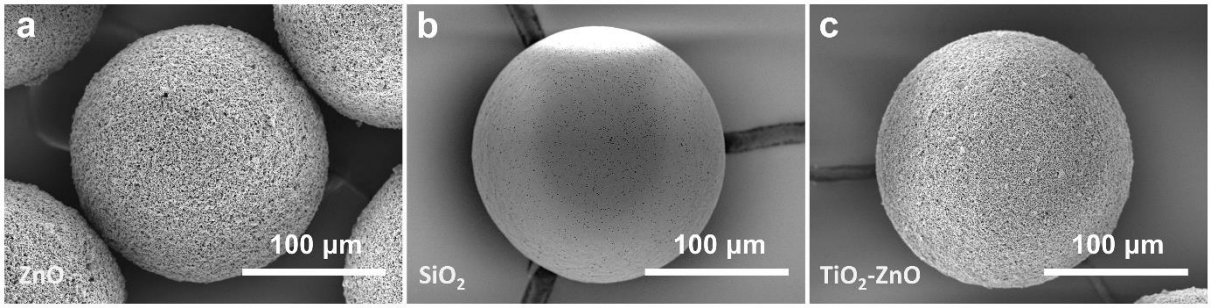

Figure S10. Highly porous supraparticles with different materials imaged by SEM. ZnO (a) and Silica (b) porous supraparticles derived from ZnO/PS (ZnO:PS=1:5) and SiO_2/PS (SiO_2:PS=1:1) binary nanoparticle suspensions. (c) Binary TiO_2-ZnO porous supraparticles made from TiO_2/ZnO/PS (TiO_2:ZnO:PS=1:1:10) ternary suspensions.

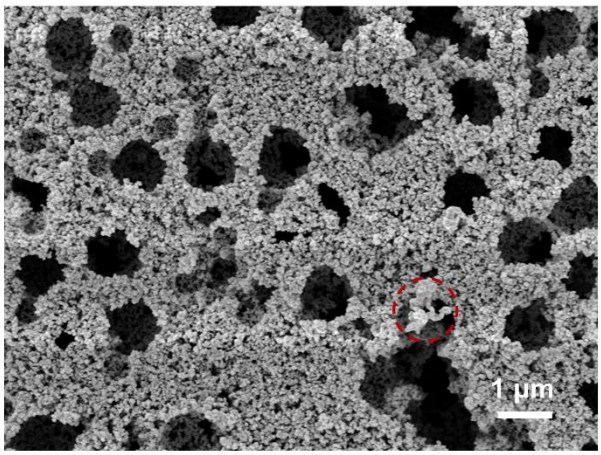

Figure S11. SEM image of the surface of porous TiO_2 supraparticle with some nanofilaments remaining (as shown in the red circle).

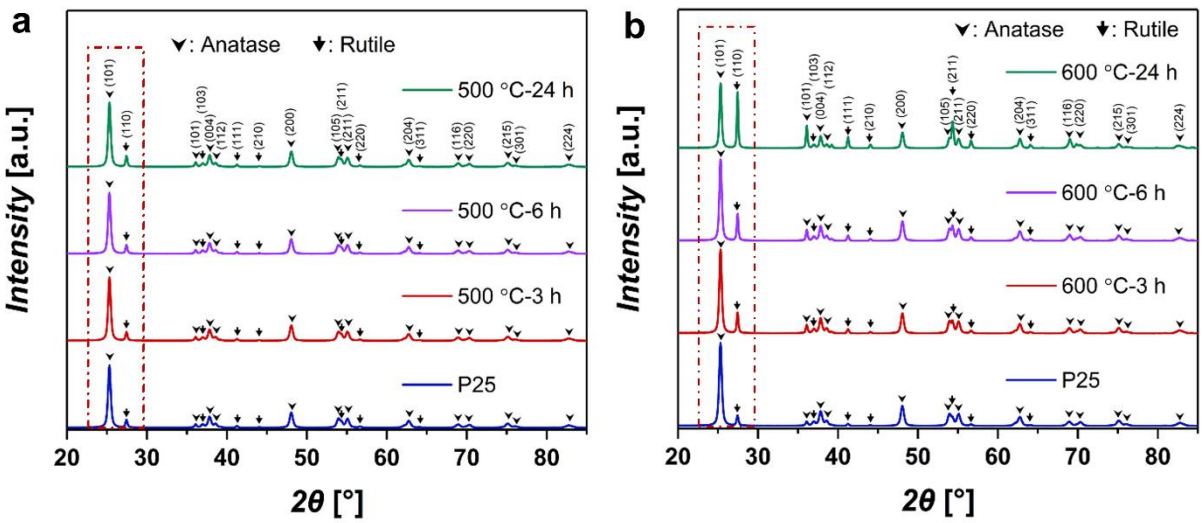

Figure S12. XRD patterns of TiO_2 (P25) nanoparticles with and without calcination. (a) Comparison of normalized XRD patterns for P25 and P25 calcination at 500 °C for 3 h, 6 h and 24 h. (b) Comparison of normalized XRD patterns for P25 and P25 calcination at 600 °C for 3 h, 6 h and 24 h.

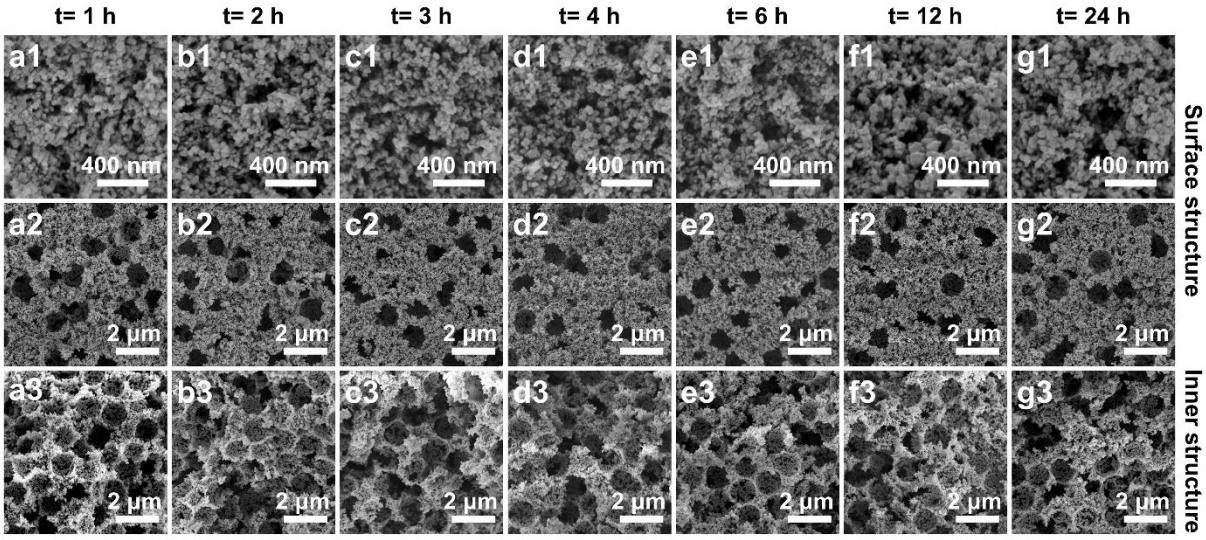

Figure S13. SEM images for the mesopore (1) and macropore (2) structure of surface, and inner structure (3) after calcination of supraparticles obtained by calcining the binary supraparticle (R=1:5) at 400 °C. The calcination times are 1 h (a1, a2, a3), 2 h (b1, b2, b3), 3 h (c1, c2, c3), 4 h (d1, d2, d3), 6 h (e1, e2, e3), 12 h (f1, f2, f3), and 24 h (g1, g2, g3), respectively, the daimeter of PS particles was about 1.25 μm.

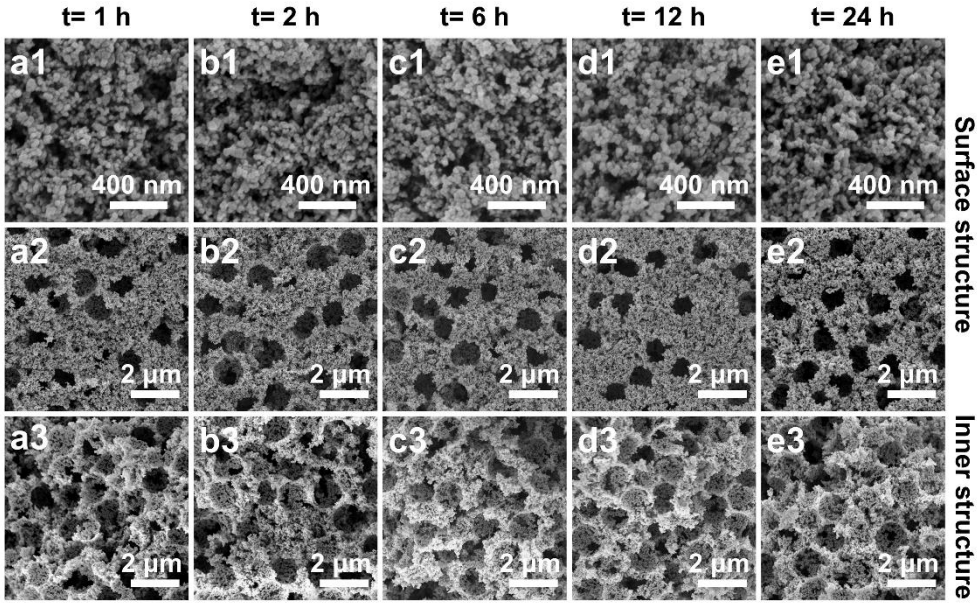

Figure S14. SEM images for the mesopore (1) and macropore (2) structure of surface, and inner structure (3) after calcination of supraparticles obtained by calcining the binary supraparticle (R=1:5) at 500 °C. The calcination times are 1 h (a1, a2, a3), 2 h (b1, b2, b3), 6 h (c1, c2, c3), 12 h (d1, d2, d3), and 24 h (e1, e2, e3), respectively, the diameter of PS particles was about 1.25 μm.

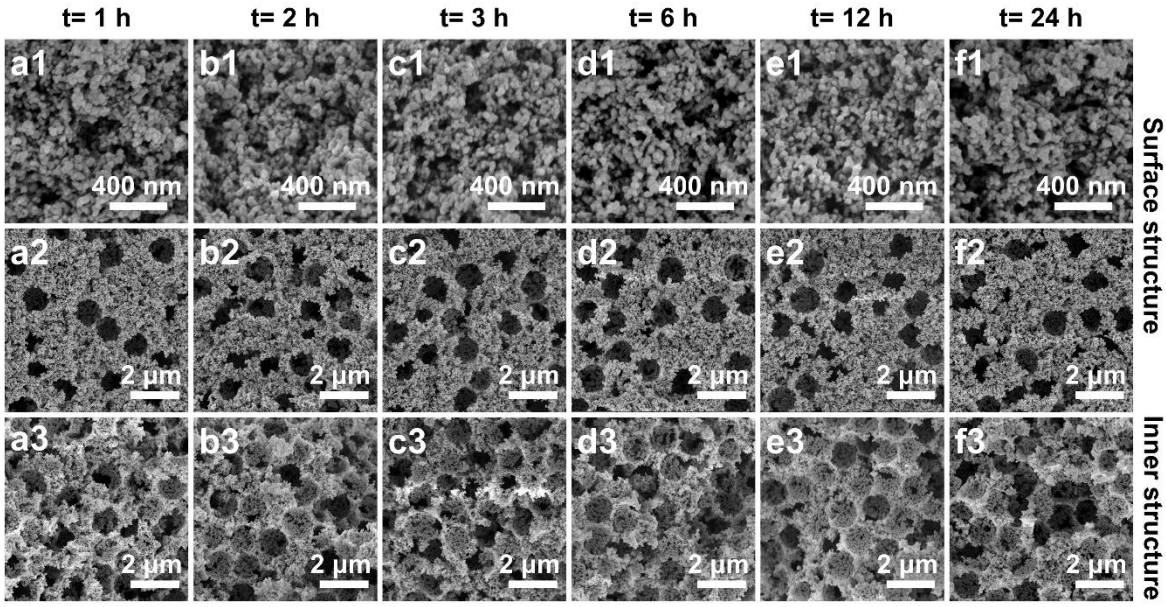

Figure S15. SEM images for the mesopore (1) and macropore (2) structure of surface, and inner structure (3) after calcination of supraparticles obtained by calcining the binary supraparticle (R=1:5) at 600 °C. The calcination times are 1 h (a1, a2, a3), 2 h (b1, b2, b3), 3 h (c1, c2, c3), 6 h (d1, d2, d3), 12 h (e1, e2, e3), and 24 h (f1, f2, f3) respectively, the diameter of PS particles was about 1.25 μm.

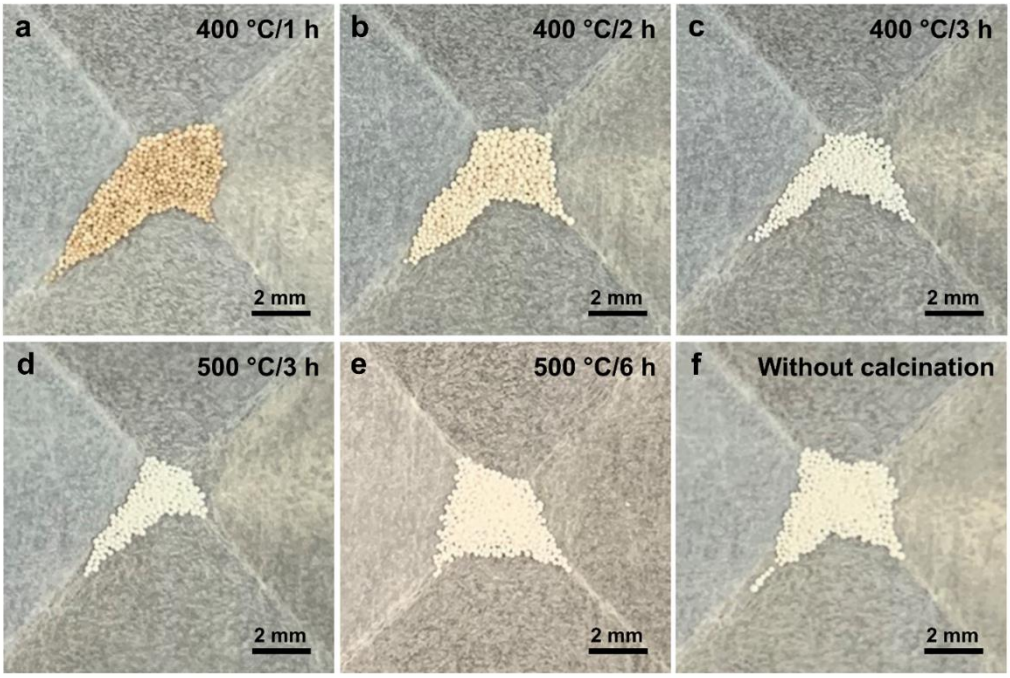

Figure S16. Optical images of TiO_2 supraparticles obtained after different calcination processes. (a-c) TiO_2 supraparticles obtained after calcination conducted at 400 °C for 1 h (a), 2 h (b), and 3 h (c), respectively. (d-e) TiO_2 supraparticles obtained after calcination conducted at 500 °C for 1 h (d), and 2 h (e). (f) TiO_2-PS binary supraparticles without calcination.

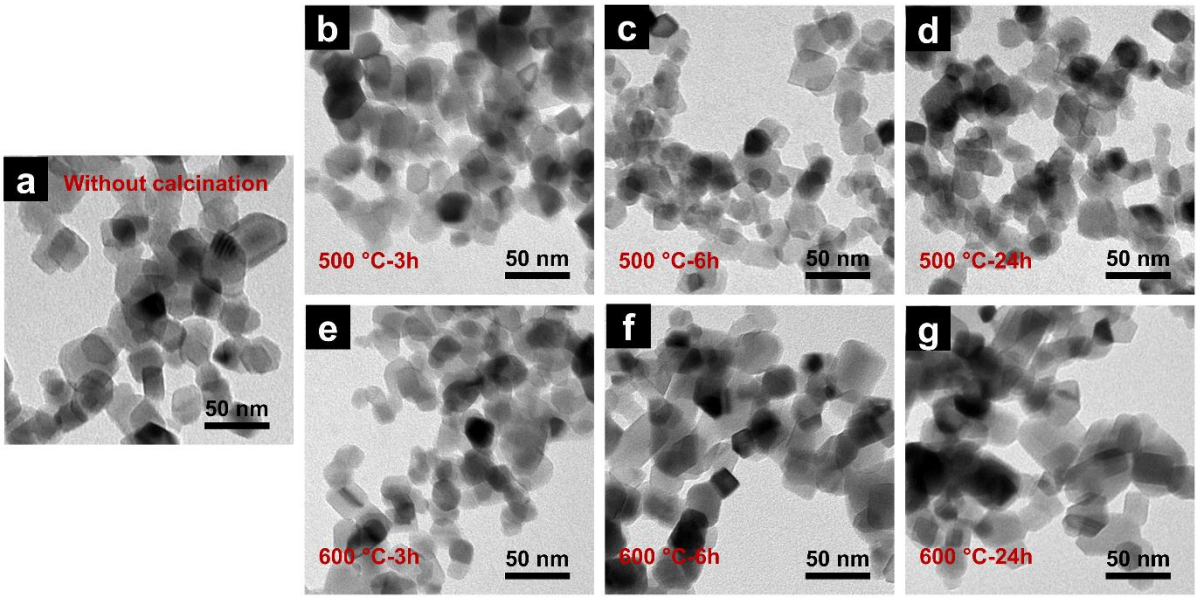

Figure S17. TEM images of TiO_2 (P25) nanoparticles with and without calcination. (a) TiO_2 nanoparticles without calcination. (b-d) TiO_2 nanoparticles experienced a calcination conducted at 500 °C for 3 h, 6 h, and 24 h, respectively. (e-g) TiO_2 nanoparticles experienced a calcination conducted at 500 °C for 3 h, 6 h, and 24 h, respectively.

Table S1. PS volume ratio in binary supraparticles and corresponding porosity of the final TiO_2 supraparticles obtained by evaporating droplets with different volume ratios R of TiO_2 to PS.

Volume ratio R (TiO_2 : PS)	PS volume ratio in binary supraparticles (%)	Porosity of TiO_2 supraparticles (%)
1:0	0	65.8 ± 0.9
1:1	18.9 ± 0.6	74.7 ± 0.7
1:3	35.3 ± 0.9	83.4 ± 0.6
1:5	45.1 ± 1.8	89.5 ± 0.6
1:7	49.3 ± 1.8	91.6 ± 1
1:9	49.4 ± 0.9	92.1 ± 0.6